Editors' Suggestion

Quantifying Energy Conversion in Higher-Order Phase Space Density Moments in Plasmas

Paul A. Cassak* and M. Hasan Barbhuiya
Department of Physics and Astronomy and the Center for KINETIC Plasma Physics, West Virginia University, Morgantown, West Virginia 26506, USA

Haoming Liang
Center for Space Plasma and Aeronomic Research, University of Alabama in Huntsville, Huntsville, Alabama 35899, USA

Matthew R. Argall
Space Science Center, Institute for the Study of Earth, Oceans, and Space, University of New Hampshire, Durham, New Hampshire 03824, USA

(Received 5 October 2022; revised 9 January 2023; accepted 24 January 2023; published 22 February 2023)

Weakly collisional and collisionless plasmas are typically far from local thermodynamic equilibrium (LTE), and understanding energy conversion in such systems is a forefront research problem. The standard approach is to investigate changes in internal (thermal) energy and density, but this omits energy conversion that changes any higher-order moments of the phase space density. In this Letter, we calculate from first principles the energy conversion associated with all higher moments of the phase space density for systems not in LTE. Particle-in-cell simulations of collisionless magnetic reconnection reveal that energy conversion associated with higher-order moments can be locally significant. The results may be useful in numerous plasma settings, such as reconnection, turbulence, shocks, and wave-particle interactions in heliospheric, planetary, and astrophysical plasmas.

DOI: 10.1103/PhysRevLett.130.085201

Energy conversion is largely well understood for systems with initial and final states in or near local thermodynamic equilibrium (LTE) [1,2]. However, energy conversion in systems far from LTE, such as weakly collisional or collisionless plasmas endemic to many space and astrophysical environments, remains a forefront research area [3,4].

For a species σ not in LTE, internal moments of the phase space density f_σ are defined as f_σ multiplied by powers of components of $\mathbf{v}'_\sigma$ and integrated over all velocity space. Here, the random velocity is $\mathbf{v}'_\sigma = \mathbf{v} - \mathbf{u}_\sigma$, velocity space coordinate is $\mathbf{v}$, bulk flow velocity is $\mathbf{u}_\sigma = (1/n_\sigma)\int f_\sigma \mathbf{v} d^3v$, and number density is $n_\sigma = \int f_\sigma d^3v$. A standard approach to study energy conversion in plasmas [5–27] centers on the first few internal moments. Compressional work describes changes to n_σ, i.e., the zeroth internal moment of f_σ, described by the continuity equation [5,28]. The internal energy per particle $\mathcal{E}_{\sigma,\mathrm{int}} = (3/2)k_B\mathcal{T}_\sigma$, i.e., the second internal moment of f_σ divided by n_σ, can change due to compressional heating by work $-\mathcal{P}_\sigma(\nabla\cdot\mathbf{u}_\sigma)$, incompressional heating via the remainder of the pressure-strain interaction (called Pi-D [5]), heat flux, or collisions, according to [2,5,28]

$$\frac{3}{2}n_\sigma k_B\frac{d\mathcal{T}_\sigma}{dt} = -(\mathbf{P}_\sigma\cdot\nabla)\cdot\mathbf{u}_\sigma - \nabla\cdot\mathbf{q}_\sigma + n_\sigma\dot{Q}_{\sigma,\mathrm{coll,inter}}. \quad (1)$$

Here, the elements of the pressure tensor $\mathbf{P}_\sigma$ are $P_{\sigma,jk} = m_\sigma\int v'_{\sigma j}v'_{\sigma k}f_\sigma d^3v$, temperature tensor is $\mathbf{T}_\sigma = \mathbf{P}_\sigma/n_\sigma k_B$, effective pressure is $\mathcal{P}_\sigma = (1/3)\mathrm{tr}[\mathbf{P}_\sigma]$, effective temperature is $\mathcal{T}_\sigma = \mathcal{P}_\sigma/n_\sigma k_B = (m_\sigma/3n_\sigma k_B)\int v'^2_\sigma f_\sigma d^3v$, vector heat flux density is $\mathbf{q}_\sigma = \int(1/2)m_\sigma v'^2_\sigma\mathbf{v}'_\sigma f_\sigma d^3v$, and volumetric heating rate per particle due to interspecies collisions is $\dot{Q}_{\sigma,\mathrm{coll,inter}} = (1/n_\sigma)\int(1/2)m_\sigma v'^2_\sigma\times\sum_{\sigma'}C_{\mathrm{inter}}[f_\sigma,f_{\sigma'}]d^3v$, where the interspecies collision operator is $C_{\mathrm{inter}}[f_\sigma,f_{\sigma'}]$, k_B is Boltzmann's constant, m_σ is the constituent mass, and $d/dt = \partial/\partial t + \mathbf{u}_\sigma\cdot\nabla$ is the convective derivative.

There is an energy conversion channel beyond those discussed thus far. f_σ has an infinite number of internal moments that are all treated on equal footing. While Eq. (1) includes the impact of off-diagonal pressure tensor elements and heat flux on $\mathcal{E}_{\sigma,\mathrm{int}}$, any energy conversion associated with time evolution of all other internal moments themselves is not contained in the continuity equation or Eq. (1).

Studies have addressed time evolution of other moments and their contribution to energy conversion. The evolution of anisotropic pressures has been studied [12,14,29–36]. Other approaches capture the effect of all moments of f_σ. Linearizing f_σ around its equilibrium in kinetic theory and gyrokinetics reveals the so-called free energy [37–39],

which quantifies non-LTE energy conversion into mechanical or magnetic energy [37]. It is associated with the phase space cascade of entropy that can lead to dissipation [40]. The velocity space cascade has been studied without linearizing f_σ [17,41–43]. In another approach, changes to bulk kinetic energy are quantified kinetically using field-particle correlations [44–53].

In this Letter, we use a first-principles theory to quantify energy conversion associated with all internal moments. We show this energy conversion is physically associated with changing the velocity space shape of f_σ. There are three important ingredients. First, the key quantity is kinetic entropy [2,54–57] rather than energy. Second, we employ the decomposition of kinetic entropy into position and velocity space kinetic entropy [58,59]. Third, we employ the so-called relative entropy [55,56,60]. Our analysis was performed independently, but we found it is similar to treatments in chemical physics of dilute gases [55] and quantum statistical mechanics [61]. The novelty of our analysis stems from using the decomposition of kinetic entropy and significant differences in interpretation than in previous work. We employ a particle-in-cell (PIC) simulation of collisionless magnetic reconnection, revealing energy conversion associated with higher-order moments can be locally significant.

We first derive an expression for the rate of energy conversion associated with non-LTE internal moments of f_σ, emphasizing departures from the treatment in Ref. [55]. We assume a classical (nonrelativistic, nonquantum) three-dimensional (3D) system of infinite volume or in a thermally insulated domain with a fixed number N_σ of monatomic particles. The kinetic entropy density s_σ associated with f_σ is [62]

$$s_\sigma = -k_B \int f_\sigma \ln\left(\frac{f_\sigma \Delta^3 r_\sigma \Delta^3 v_\sigma}{N_\sigma}\right) d^3v, \tag{2}$$

where the integral is over all velocity space, and $\Delta^3 r_\sigma$ and $\Delta^3 v_\sigma$ are position space and velocity space volume elements in phase space, respectively [59,63,64]. In the comoving (Lagrangian) frame, s_σ evolves according to ([55] and Supplemental Material Sec. A [65])

$$\frac{d}{dt}\left(\frac{s_\sigma}{n_\sigma}\right) + \frac{\nabla \cdot \mathcal{J}_{\sigma,\mathrm{th}}}{n_\sigma} = \frac{\dot{s}_{\sigma,\mathrm{coll}}}{n_\sigma}, \tag{3}$$

where $\mathcal{J}_{\sigma,\mathrm{th}}$ is thermal kinetic entropy density flux and $\dot{s}_{\sigma,\mathrm{coll}}$ is local time rate of change of kinetic entropy density through collisions, defined in Eqs. (S.4) and (S.3) [65], respectively. We note that Eq. (3) has no explicit dependence on body forces including gravitational and electromagnetic forces, which implies they do not directly change internal moments of f_σ. Equation (1) exemplifies this for the special case of internal energy.

In a key departure from Ref. [55], we decompose kinetic entropy density s_σ into a position space kinetic entropy density $s_{\sigma p}$ and velocity space kinetic entropy density $s_{\sigma v}$, with $s_\sigma = s_{\sigma p} + s_{\sigma v}$, as [58,59]

$$s_{\sigma p} = -k_B n_\sigma \ln\left(\frac{n_\sigma \Delta^3 r_\sigma}{N_\sigma}\right), \tag{4a}$$

$$s_{\sigma v} = -k_B \int f_\sigma \ln\left(\frac{f_\sigma \Delta^3 v_\sigma}{n_\sigma}\right) d^3v. \tag{4b}$$

A direct calculation (see Supplemental Material Secs. B–D [65]) of the terms on the left side of Eq. (3) using Eqs. (4a) and (4b) gives

$$\frac{d}{dt}\left(\frac{s_{\sigma p}}{n_\sigma}\right) = \frac{1}{\mathcal{T}_\sigma}\frac{d\mathcal{W}_\sigma}{dt}, \tag{5a}$$

$$\frac{d}{dt}\left(\frac{s_{\sigma v}}{n_\sigma}\right) = \frac{1}{\mathcal{T}_\sigma}\frac{d\mathcal{E}_{\sigma,\mathrm{int}}}{dt} + \frac{d}{dt}\left(\frac{s_{\sigma v,\mathrm{rel}}}{n_\sigma}\right), \tag{5b}$$

$$\frac{\nabla \cdot \mathcal{J}_{\sigma,\mathrm{th}}}{n_\sigma} = -\frac{1}{\mathcal{T}_\sigma}\frac{d\mathcal{Q}_\sigma}{dt} + \frac{(\nabla \cdot \mathcal{J}_{\sigma,\mathrm{th}})_{\mathrm{rel}}}{n_\sigma}, \tag{5c}$$

where $d\mathcal{W}_\sigma = \mathcal{P}_\sigma d(1/n_\sigma)$ is the compressional work per particle done by the system, $d\mathcal{E}_{\sigma,\mathrm{int}} = (3/2)k_B d\mathcal{T}_\sigma$ is the increment in internal energy per particle, and $d\mathcal{Q}_\sigma/dt = [-\nabla \cdot \mathbf{q}_\sigma - (\mathbf{P}_\sigma \cdot \nabla) \cdot \mathbf{u}_\sigma + \mathcal{P}_\sigma(\nabla \cdot \mathbf{u}_\sigma)]/n_\sigma$ is the (thermodynamic) heating rate per particle from sources other than compression that can change the effective temperature [see Eq. (1)]. Finally, $s_{\sigma v,\mathrm{rel}}$ is the relative entropy density and $(\nabla \cdot \mathcal{J}_{\sigma,\mathrm{th}})_{\mathrm{rel}}$ is the thermal relative entropy density flux divergence, given by

$$s_{\sigma v,\mathrm{rel}} = -k_B \int f_\sigma \ln\left(\frac{f_\sigma}{f_{\sigma M}}\right) d^3v, \tag{6}$$

$$(\nabla \cdot \mathcal{J}_{\sigma,\mathrm{th}})_{\mathrm{rel}} = -k_B \int [\nabla \cdot (\mathbf{v}'_\sigma f_\sigma)] \ln\left(\frac{f_\sigma}{f_{\sigma M}}\right) d^3v, \tag{7}$$

and the "Maxwellianized" phase space density $f_{\sigma M}$ associated with f_σ is [60]

$$f_{\sigma M} = n_\sigma \left(\frac{m_\sigma}{2\pi k_B \mathcal{T}_\sigma}\right)^{3/2} e^{-m_\sigma(\mathbf{v}-\mathbf{u}_\sigma)^2/2k_B\mathcal{T}_\sigma}, \tag{8}$$

where n_σ, $\mathbf{u}_\sigma$, and $\mathcal{T}_\sigma$ are based on f_σ. (Reference [55] used a more general reference phase space density than $f_{\sigma M}$, so our choice is a special case of theirs.)

Equations (5a)–(5c) have important implications, and our interpretation greatly departs from Ref. [55]. Ignoring the relative terms in Eqs. (5b) and (5c), we see Eq. (3) (scaled by the effective temperature) inherently contains information about work, internal energy, and thermodynamic heat as captured by the continuity equation and

Eq. (1). This suggests the relative terms describe energy conversion associated with all internal moments beyond the second moment.

We therefore define increments of relative energy per particle $d\mathcal{E}_{\sigma,\mathrm{rel}}$ and relative heat per particle $d\mathcal{Q}_{\sigma,\mathrm{rel}}$ by

$$\frac{d\mathcal{E}_{\sigma,\mathrm{rel}}}{dt} = \mathcal{T}_\sigma \frac{d(s_{\sigma v,\mathrm{rel}}/n_\sigma)}{dt}, \tag{9a}$$

$$\frac{d\mathcal{Q}_{\sigma,\mathrm{rel}}}{dt} = -\mathcal{T}_\sigma \frac{(\nabla\cdot\mathcal{J}_{\sigma,\mathrm{th}})_{\mathrm{rel}}}{n_\sigma}. \tag{9b}$$

Further defining energy increments per particle in all internal moments at and above the second moment as $d\mathcal{E}_{\sigma,\mathrm{gen}} = d\mathcal{E}_{\sigma,\mathrm{int}} + d\mathcal{E}_{\sigma,\mathrm{rel}}$ and generalized heat per particle as $d\mathcal{Q}_{\sigma,\mathrm{gen}} = d\mathcal{Q}_\sigma + d\mathcal{Q}_{\sigma,\mathrm{rel}}$, Eqs. (3)–(5c), (9a), and (9b) take on the simple form

$$\frac{d\mathcal{W}_\sigma}{dt} + \frac{d\mathcal{E}_{\sigma,\mathrm{gen}}}{dt} = \frac{d\mathcal{Q}_{\sigma,\mathrm{gen}}}{dt} + \dot{\mathcal{Q}}_{\sigma,\mathrm{coll}}, \tag{10}$$

where $\dot{\mathcal{Q}}_{\sigma,\mathrm{coll}} = \mathcal{T}_\sigma \dot{s}_{\sigma,\mathrm{coll}}/n_\sigma$. Equation (10) generalizes Eq. (1), which contains energy conversion associated with only density and effective temperature, as opposed to all internal moments of f_σ. This interpretation is a significant departure from Ref. [55].

We now provide a physical interpretation, which requires understanding energy conversion via its impact on f_σ. Work per particle $d\mathcal{W}_\sigma = \mathcal{P}_\sigma d(1/n_\sigma)$ changes the zeroth moment of f_σ. This is depicted graphically in Fig. 1, where two velocity space dimensions of f_σ are sketched. The top row shows a process taking a Maxwellianized f_σ from an initial to final state. The intensification of colors denote a change in f_σ and therefore n_σ. Similarly, $d\mathcal{E}_{\sigma,\mathrm{int}}$ is associated with changes to the second internal moment of f_σ, depicted in the second row of Fig. 1 for a process that

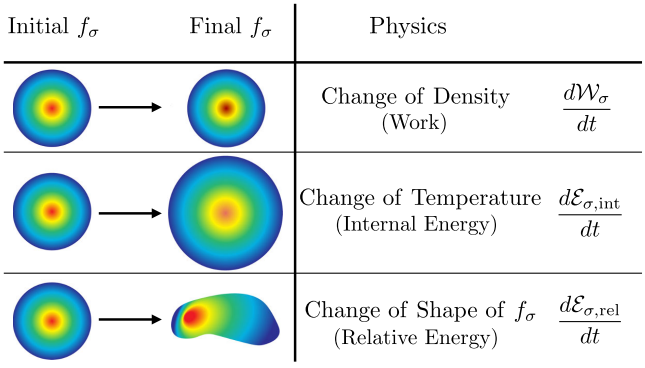

FIG. 1. Schematic showing energy conversion channels according to their impact on the phase space density f_σ. The initial f_σ is depicted as Maxwellian for illustrative purposes on the left. The final f_σ is to their right. The descriptions of the changes in f_σ are to their right.

increases $\mathcal{E}_{\sigma,\mathrm{int}}$, i.e., the Maxwellianized f_σ spreads in velocity space.

To interpret $d\mathcal{E}_{\sigma,\mathrm{rel}}$, Eq. (6) shows $s_{\sigma v,\mathrm{rel}}$ vanishes if f_σ is a Maxwellian ($f_\sigma = f_{\sigma M}$) [60]. Thus, $d\mathcal{E}_{\sigma,\mathrm{rel}}$ describes non-LTE physics. Since a Maxwellian is the highest kinetic entropy state for a fixed N_σ and $\mathcal{E}_{\sigma,\mathrm{int}}$ [54], $d(s_{\sigma v,\mathrm{rel}}/n_\sigma)/dt > 0$ implies f_σ evolves toward Maxwellianity in the comoving frame, associated with $d\mathcal{E}_{\sigma,\mathrm{rel}} > 0$, while $d(s_{\sigma v,\mathrm{rel}}/n_\sigma)/dt < 0$ implies f_σ evolves away from Maxwellianity and $d\mathcal{E}_{\sigma,\mathrm{rel}} < 0$. A process changing the shape of f_σ is depicted in the third row of Fig. 1, where f_σ is initially Maxwellian and finally it is not.

A concrete example showing that $d\mathcal{E}_{\sigma,\mathrm{rel}}$ is associated with f_σ changing shape is provided in Supplemental Material Sec. E [65]. $d\mathcal{E}_{\sigma,\mathrm{rel}}$ is calculated analytically for a bi-Maxwellian distribution with converging flow. It is shown that the evolution of f_σ is consistent with the interpretation in the previous paragraph.

Collisions directly change the shape of f_σ, so $d\mathcal{E}_{\sigma,\mathrm{rel}}$ includes irreversible contributions if collisions are present. However, since f_σ can change shape even in the perfectly collisionless limit, $d\mathcal{E}_{\sigma,\mathrm{rel}}$ also contains reversible effects. Thus, the term is not purely irreversible as previously suggested [55].

$d\mathcal{Q}_\sigma$ describes non-Maxwellian features of f_σ that cause a flux of energy per particle that changes $\mathcal{T}_\sigma$ [see Eq. (1)]. $d\mathcal{Q}_{\sigma,\mathrm{rel}}$ is analogous: non-Maxwellian features in higher-order internal moments produce a flux that modifies internal moments of f_σ other than n_σ and $\mathcal{T}_\sigma$. $\dot{\mathcal{Q}}_{\sigma,\mathrm{coll}}$ describes both intra- and interspecies collisions, as opposed to solely interspecies arising in Eq. (1). This is because both collision types can change higher-order internal moments of f_σ, while elastic intraspecies collisions conserve energy.

We demonstrate key results of the theory using simulations of reconnection. Data are from the simulation in Ref. [27]. The code and numerical aspects are discussed there and in Supplemental Material Sec. F [65]. The out-of-plane current density J_z around a reconnection X line at (x_0, y_0) is in Fig. 2(a), with reversing magnetic field lines in black and electron streamline segments in orange, revealing typical profiles.

We first confirm relative energy changes are related to f_σ evolving toward or away from LTE. Figure 2(b) shows the electron entropy-based Kaufmann and Paterson non-Maxwellianity $\bar{M}_{e,\mathrm{KP}} = (s_{eM} - s_e)/[(3/2)k_B n_e]$ [63,89], where s_e comes from Eq. (2) based on f_e, while s_{eM} comes from Eq. (2) based on f_{eM} in Eq. (8). It is a measure of the temporally and spatially local departure from LTE. Figure 2(e) is the rate of relative energy per particle $d\mathcal{E}_{e,\mathrm{rel}}/dt$. Figures 2(i)–2(l) are reduced electron phase space densities $f_e(v_x, v_z)$ at the four color-coded x's along a streamline in Fig. 2(b).

$\bar{M}_{e,\mathrm{KP}}$ and $d\mathcal{E}_{e,\mathrm{rel}}/dt$ together reveal whether f_σ is locally in LTE [Fig. 2(b)] and whether it is evolving toward or away from LTE [Fig. 2(e)]. Just upstream of the electron

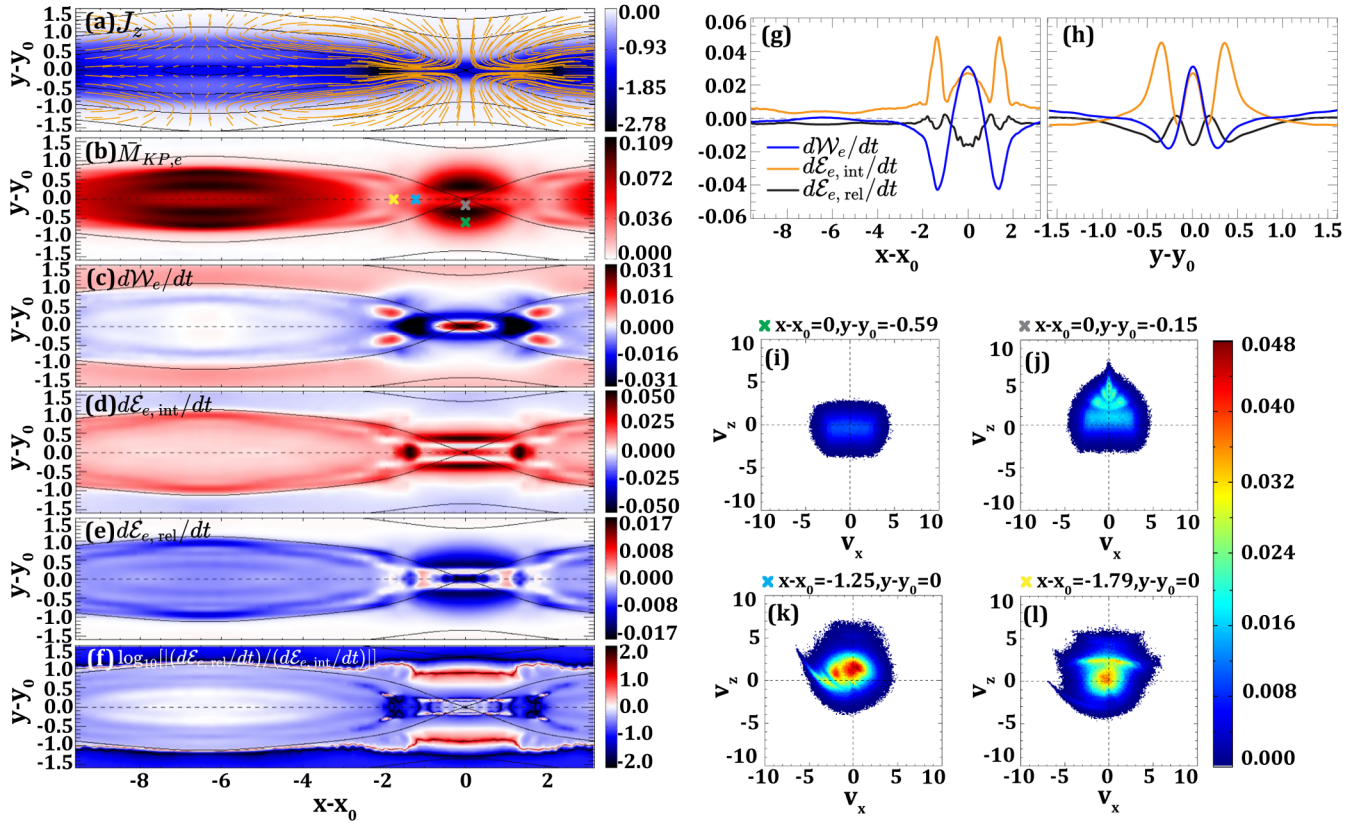

FIG. 2. Electron energy conversion in a PIC simulation of magnetic reconnection. (a) Out-of-plane current density J_z, with projections of magnetic field lines and segments of electron velocity streamlines overplotted in black and orange, respectively. (b) Electron entropy-based non-Maxwellianity $\bar{M}_{\mathrm{KP},e}$. Time rates of change per particle of (c) work $d\mathcal{W}_e/dt$, (d) internal energy $d\mathcal{E}_{e,\mathrm{int}}/dt$, and (e) relative energy $d\mathcal{E}_{e,\mathrm{rel}}/dt$. (f) $\log_{10}[|(d\mathcal{E}_{e,\mathrm{rel}}/dt)/(d\mathcal{E}_{e,\mathrm{int}}/dt)|]$. 1D cuts of the terms in (c)–(e) in the (g) x and (h) y directions. (i)–(l) Reduced electron phase space density $f_e(v_x, v_z)$ at locations denoted by the colored x's at the top left of the plots corresponding to the x's in (b) along a streamline.

diffusion region (EDR) ($|x-x_0|<1, 0.45<|y-y_0|<1$), electrons get trapped by the upstream magnetic field [34], so f_e becomes non-Maxwellian [dark red in Fig. 2(b)], with f_e elongated in the parallel direction [Fig. 2(i)]. Thus, in the comoving frame, as a fluid element convects toward the X line from upstream, f_e evolves away from Maxwellianity, consistent with Fig. 2(e), where $d\mathcal{E}_{e,\mathrm{rel}}/dt<0$. Continuing toward the X line, f_e develops striations [Fig. 2(j)] due to electrons becoming demagnetized in the reversed magnetic field [90,91]. This is associated with evolution away from LTE [blue in Fig. 2(e)]. Downstream of the X line, there is a red patch in Fig. 2(e) at $|x-x_0|\simeq 1.25$, $|y-y_0|\simeq 0$ where electrons thermalize (Maxwellianize) [92,93], which is seen in f_e [Fig. 2(k)]. Just downstream from there ($|x-x_0|\simeq 1.8$), f_e evolves away from LTE where electrons begin to remagnetize at the downstream edge of the EDR [92,94] [Fig. 2(l)]. These results confirm the sign of $d\mathcal{E}_{\sigma,\mathrm{rel}}$ identifies whether f_σ changes shape toward or away from LTE in the comoving frame.

Next, we demonstrate the quantitative importance of relative energy. Rates of work and internal energy per particle are shown in Figs. 2(c) and 2(d), respectively. Cuts of these quantities through the X line in the horizontal and vertical directions, along with $d\mathcal{E}_{e,\mathrm{rel}}/dt$, are plotted in Figs. 2(g) and 2(h), respectively. At the X line, the values are 0.031, 0.027, and −0.016, respectively, in normalized code units. Their sum, 0.042, is the total rate of energy per particle going into internal moments of electrons. To see that relative energy is important, the standard approach using Eq. (1) would say the energy rate going into changing n_e and $\mathcal{T}_e$ is $0.031+0.027=0.058$, 38% higher than the total rate when relative energy is included, which is a significant difference.

To assess its importance in other locations, Fig. 2(f) shows $\log_{10}[|(d\mathcal{E}_{e,\mathrm{rel}}/dt)/(d\mathcal{E}_{e,\mathrm{int}}/dt)|]$, with a color bar saturated at ± 2 to better reveal details. Where internal and relative energy changes are comparable are white. Locations where $|d\mathcal{E}_{e,\mathrm{rel}}|$ exceeds $|d\mathcal{E}_{e,\mathrm{int}}|$ are red, especially just upstream of the EDR. In the deep blue regions, $|d\mathcal{E}_{e,\mathrm{rel}}|\ll|d\mathcal{E}_{e,\mathrm{int}}|$. In the light blue regions, including much of the EDR and island, $|d\mathcal{E}_{e,\mathrm{rel}}|$ is at least 20% of the magnitude of $|d\mathcal{E}_{e,\mathrm{int}}|$. Thus, energy conversion associated with non-LTE internal moments in reconnection is broadly non-negligible and can be locally significant or even dominant.

We conclude with implications of the present results. First, the theory applies for systems arbitrarily far from LTE, so it could lead to significant advances compared to manifestly perturbative theories [1,2,39]. An extensive comparison to previous work is in Supplemental Material Sec. G [65]. For a physical process that changes both internal energy and higher-order moments, the theory captures both and allows each to be calculated separately. Since the theory contains all internal moments of f_σ, it overcomes the closure problem.

It is important to note that internal energy per particle $\mathcal{E}_{\sigma,\mathrm{int}}$ is a state variable, meaning it is history independent, but relative energy per particle $\mathcal{E}_{\sigma,\mathrm{rel}}$ is not [see Eq. (9a)]. Only in special cases can relative energy per particle $\mathcal{E}_{\sigma,\mathrm{rel}}$ be calculated from f_σ at a particular time. Rather, only the increment $d\mathcal{E}_{\sigma,\mathrm{rel}}$ has an instantaneous physical meaning. This was pointed out in Ref. [55] and used as motivation to not employ relative entropy per particle because they sought a thermodynamic theory of irreversible processes. Our interpretation is distinctly different; we argue relative energy per particle not being a state variable reflects the physical consequence that changing the shape of f_σ is typically history dependent. Thus, a description retaining this history dependence is crucial for quantifying energy conversion into non-LTE internal moments.

Our results reveal that the standard treatment of energy conversion in Eq. (1) needs to be expanded to accurately describe energy conservation when not in LTE. Since Eq. (1) is equivalent to the first law of thermodynamics, we argue Eq. (10) is its kinetic theory generalization, which we dub "the first law of kinetic theory."

A flow chart depicting energy conversion in non-LTE systems is in Fig. 3. Black arrows denote energy conversion contained in thermodynamics, namely, conversion between heat, work, and internal energy, plus collisions. Red arrows are for relative energy and heat associated with non-LTE internal moments of f_σ. The dashed light blue arrow denotes coupling between relative energy and thermodynamic heat through the vector heat flux density and Pi-D.

We expect the results to be useful when f_σ is reliably measured, such as PIC and Vlasov or Boltzmann plasma simulations and satellite observations [95,96]. Satellites measure f_σ with spatiotemporal resolution sufficient to take gradients [97,98] and compute kinetic entropy [64]. The theory may advance efforts using machine learning to parametrize kinetic corrections to transport terms in fluid models [99]. Generalizations of the present result may be useful beyond plasma physics, such as many-body astrophysics [100], micro- and nanofluidics [101,102], and quantum entanglement [61].

There are limitations of the present work. Each restriction to the theory listed before Eq. (2) could be relaxed. Relative energy describes energy conversion associated with all non-LTE internal moments, but does not identify which of the individual non-LTE internal moments

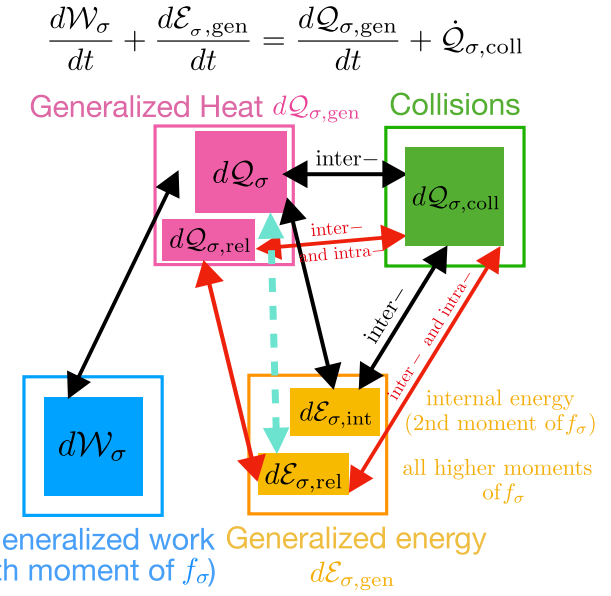

FIG. 3. Sketch illustrating energy conversion from Eq. (10). Arrows show conversion channels between work (blue), heat (pink), energy (orange), and collisions (green), with standard channels in black and relative channels in red. The light blue dashed arrow signifies how the relative terms couple to thermodynamic terms.

contribute; it would be interesting to address this in future work, likely in context of recent theories of the velocity space cascade [41] and/or Casimir invariants [103]. There are settings for which $f_{\sigma M}$ is not the appropriate reference for f_σ [104,105]. Reference [55] employs a more general reference f_σ than we use here; it would be interesting to generalize the results for more general plasma-relevant forms.

The data used in Fig. 2 are publicly available from the Zenodo repository [106].

The authors acknowledge helpful conversations with Amitava Bhattacharjee, Ned Flagg, the late Leo Golubovic, Greg Good, Colby Haggerty, David Levermore, Bill Matthaeus, Earl Scime, Mike Shay, Marc Swisdak, Eitan Tadmor, Thanos Tzavaras, and especially Art Weldon. The authors gratefully acknowledge support from NSF Grant No. PHY-1804428 (P. A. C.), NSF Grant No. AGS-1602769 (P. A. C.), NASA Grant No. 80NSSC19M0146 (P. A. C.), DOE Award No. DE-SC0020294 (P. A. C.), NASA Grant No. SV4-84017 (H. L.), NSF Grant No. OIA-1655280 (H. L.), NASA Grants No. 80GSFC19C0027 (H. L.), No. 80NSSC20K1783 (H. L.), No. 80NSSC21K0003 (H. L.), and NASA Contract No. NNG04EB99C (M. R. A.). This research uses resources of the National Energy Research Scientific Computing Center (NERSC), a DOE Office of Science User Facility supported by the Office of Science of the U.S. Department of Energy under Award No. DE-AC02-05CH11231.

*Paul.Cassak@mail.wvu.edu

[1] S. Chapman and T. G. Cowling, *The Mathematical Theory of Non-Uniform Gases. An Account of the Kinetic Theory of Viscosity, Thermal Conduction and Diffusion in Gases*, 3rd ed. (Cambridge University Press, Cambridge, England, 1970).

[2] D. Jou, G. Lebon, and J. Casas-Vázquez, *Extended Irreversible Thermodynamics*, 4th ed. (Springer, Dordrecht, 2010).

[3] G. G. Howes, A prospectus on kinetic heliophysics, Phys. Plasmas **24**, 055907 (2017).

[4] W. H. Matthaeus, Y. Yang, M. Wan, T. N. Parashar, R. Bandyopadhyay, A. Chasapis, O. Pezzi, and F. Valentini, Pathways to dissipation in weakly collisional plasmas, Astrophys. J. **891**, 101 (2020).

[5] Y. Yang, W. H. Matthaeus, T. N. Parashar, C. C. Haggerty, V. Roytershteyn, W. Daughton, M. Wan, Y. Shi, and S. Chen, Energy transfer, pressure tensor, and heating of kinetic plasma, Phys. Plasmas **24**, 072306 (2017).

[6] A. Chasapis, Y. Yang, W. H. Matthaeus, T. N. Parashar, C. C. Haggerty, J. L. Burch, T. E. Moore, C. J. Pollock, J. Dorelli, D. J. Gershman, R. B. Torbert, and C. T. Russell, Energy conversion and collisionless plasma dissipation channels in the turbulent magnetosheath observed by the magnetospheric multiscale mission, Astrophys. J. **862**, 32 (2018).

[7] Z. H. Zhong, X. H. Deng, M. Zhou, W. Q. Ma, R. X. Tang, Y. V. Khotyaintsev, B. L. Giles, C. T. Russell, and J. L. Burch, Energy conversion and dissipation at dipolarization fronts: A statistical overview, Geophys. Res. Lett. **46**, 12693 (2019).

[8] R. Bandyopadhyay, W. H. Matthaeus, T. N. Parashar, Y. Yang, A. Chasapis, B. L. Giles, D. J. Gershman, C. J. Pollock, C. T. Russell, R. J. Strangeway, R. B. Torbert, T. E. Moore, and J. L. Burch, Statistics of Kinetic Dissipation in the Earth's Magnetosheath: MMS Observations, Phys. Rev. Lett. **124**, 255101 (2020).

[9] R. Bandyopadhyay, A. Chasapis, W. H. Matthaeus, T. N. Parashar, C. C. Haggerty, M. A. Shay, D. J. Gershman, B. L. Giles, and J. L. Burch, Energy dissipation in turbulent reconnection, Phys. Plasmas **28**, 112305 (2021).

[10] Y. Wang, R. Bandyopadhyay, R. Chhiber, W. H. Matthaeus, A. Chasapis, Y. Yang, F. D. Wilder, D. J. Gershman, B. L. Giles, C. J. Pollock, J. Dorelli, C. T. Russell, R. J. Strangeway, R. T. Torbert, T. E. Moore, and J. L. Burch, Statistical survey of collisionless dissipation in the terrestrial magnetosheath, J. Geophys. Res. **126**, e2020JA029000 (2021).

[11] M. Zhou, H. Man, Y. Yang, Z. Zhong, and X. Deng, Measurements of energy dissipation in the electron diffusion region, Geophys. Res. Lett. **48**, e2021GL096372 (2021).

[12] D. Del Sarto, F. Pegoraro, and F. Califano, Pressure anisotropy and small spatial scales induced by velocity shear, Phys. Rev. E **93**, 053203 (2016).

[13] M. I. Sitnov, V. G. Merkin, V. Roytershteyn, and M. Swisdak, Kinetic dissipation around a dipolarization front, Geophys. Res. Lett. **45**, 4639 (2018).

[14] D. Del Sarto and F. Pegoraro, Shear-induced pressure anisotropization and correlation with fluid vorticity in a low collisionality plasma, Mon. Not. R. Astron. Soc. **475**, 181 (2018).

[15] S. Du, F. Guo, G. P. Zank, X. Li, and A. Stanier, Plasma energization in colliding magnetic flux ropes, Astrophys. J. **867**, 16 (2018).

[16] T. N. Parashar, W. H. Matthaeus, and M. A. Shay, Dependence of kinetic plasma turbulence on plasma β, Astrophys. J. Lett. **864**, L21 (2018).

[17] O. Pezzi, Y. Yang, F. Valentini, S. Servidio, A. Chasapis, W. H. Matthaeus, and P. Veltri, Energy conversion in turbulent weakly collisional plasmas: Eulerian hybrid Vlasov-Maxwell simulations, Phys. Plasmas **26**, 072301 (2019).

[18] Y. Yang, M. Wan, W. H. Matthaeus, L. Sorriso-Valvo, T. N. Parashar, Q. Lu, Y. Shi, and S. Chen, Scale dependence of energy transfer in turbulent plasma, Mon. Not. R. Astron. Soc. **482**, 4933 (2019).

[19] L. Song, M. Zhou, Y. Yi, X. Deng, Z. Zhong, and H. Man, Force and energy balance of the dipolarization front, J. Geophys. Res. **125**, e2020JA028278 (2020).

[20] S. Du, G. P. Zank, X. Li, and F. Guo, Energy dissipation and entropy in collisionless plasma, Phys. Rev. E **101**, 033208 (2020).

[21] S. Fadanelli, B. Lavraud, F. Califano, G. Cozzani, F. Finelli, and M. Sisti, Energy conversions associated with magnetic reconnection, J. Geophys. Res. **126**, e2020JA028333 (2021).

[22] G. Arró, F. Califano, and G. Lapenta, Spectral properties and energy cascade at kinetic scales in collisionless plasma turbulence, Astron. Astrophys. **668**, A33 (2022).

[23] Y. Yang, W. H. Matthaeus, S. Roy, V. Roytershteyn, T. N. Parashar, R. Bandyopadhyay, and M. Wan, Pressure–strain interaction as the energy dissipation estimate in collisionless plasma, Astrophys. J. **929**, 142 (2022).

[24] P. Hellinger, V. Montagud-Camps, L. Franci, L. Matteini, E. Papini, A. Verdini, and S. Landi, Ion-scale transition of plasma turbulence: Pressure-strain effect, Astrophys. J. **930**, 48 (2022).

[25] P. A. Cassak and M. H. Barbhuiya, Pressure-strain interaction. I. On compression, deformation, and implications for Pi-D, Phys. Plasmas **29**, 122306 (2022).

[26] P. A. Cassak, M. H. Barbhuiya, and H. A. Weldon, Pressure-strain interaction. II. Decomposition in magnetic field-aligned coordinates, Phys. Plasmas **29**, 122307 (2022).

[27] M. H. Barbhuiya and P. A. Cassak, Pressure-strain interaction. III. Particle-in-cell simulations of magnetic reconnection, Phys. Plasmas **29**, 122308 (2022).

[28] S. I. Braginskii, Transport processes in a plasma, Rev. Plasma Phys. **1**, 205 (1965).

[29] M. M. Kuznetsova, M. Hesse, and D. Winske, Kinetic quasi-viscous and bulk flow inertia effects in collisionless magnetotail reconnection, J. Geophys. Res. **103**, 199 (1998).

[30] L. Yin and D. Winske, Plasma pressure tensor effects on reconnection: Hybrid and hall-magnetohydrodynamics simulations, Phys. Plasmas **10**, 1595 (2003).

[31] J. Brackbill, A comparison of fluid and kinetic models of steady magnetic reconnection, Phys. Plasmas **18**, 032309 (2011).

[32] A. Greco, F. Valentini, S. Servidio, and W. H. Matthaeus, Inhomogeneous kinetic effects related to intermittent magnetic discontinuities, Phys. Rev. E **86**, 066405 (2012).
[33] S. Servidio, F. Valentini, F. Califano, and P. Veltri, Local Kinetic Effects in Two-Dimensional Plasma Turbulence, Phys. Rev. Lett. **108**, 045001 (2012).
[34] J. Egedal, A. Le, and W. Daughton, A review of pressure anisotropy caused by electron trapping in collisionless plasma, and its implications for magnetic reconnection, Phys. Plasmas **20**, 061201 (2013).
[35] L. Wang, A. H. Hakim, A. Bhattacharjee, and K. Germaschewski, Comparison of multi-fluid moment models with particle-in-cell simulations of collisionless magnetic reconnection, Phys. Plasmas **22**, 012108 (2015).
[36] M. Swisdak, Quantifying gyrotropy in magnetic reconnection, Geophys. Res. Lett. **43**, 43 (2016).
[37] K. Hallatschek, Thermodynamic Potential in Local Turbulence Simulations, Phys. Rev. Lett. **93**, 125001 (2004).
[38] G. G. Howes, S. C. Cowley, W. Dorland, G. W. Hammett, E. Quataert, and A. A. Schekochihin, Astrophysical gyrokinetics: Basic equations and linear theory, Astrophys. J. **651**, 590 (2006).
[39] A. Schekochihin, S. Cowley, W. Dorland, G. Hammett, G. G. Howes, E. Quataert, and T. Tatsuno, Astrophysical gyrokinetics: Kinetic and fluid turbulent cascades in magnetized weakly collisional plasmas, Astrophys. J. Suppl. Ser. **182**, 310 (2009).
[40] T. Tatsuno, W. Dorland, A. A. Schekochihin, G. G. Plunk, M. Barnes, S. C. Cowley, and G. G. Howes, Nonlinear Phase Mixing and Phase-Space Cascade of Entropy in Gyrokinetic Plasma Turbulence, Phys. Rev. Lett. **103**, 015003 (2009).
[41] S. Servidio, A. Chasapis, W. H. Matthaeus, D. Perrone, F. Valentini, T. N. Parashar, P. Veltri, D. Gershman, C. T. Russell, B. Giles, S. A. Fuselier, T. D. Phan, and J. Burch, Magnetospheric Multiscale Observation of Plasma Velocity-Space Cascade: Hermite Representation and Theory, Phys. Rev. Lett. **119**, 205101 (2017).
[42] O. Pezzi, S. Servidio, D. Perrone, F. Valentini, L. Sorriso-Valvo, A. Greco, W. Matthaeus, and P. Veltri, Velocity-space cascade in magnetized plasmas: Numerical simulations, Phys. Plasmas **25**, 060704 (2018).
[43] S. Cerri, M. W. Kunz, and F. Califano, Dual phase-space cascades in 3d hybrid-Vlasov–Maxwell turbulence, Astrophys. J. Lett. **856**, L13 (2018).
[44] K. G. Klein and G. G. Howes, Measuring collisionless damping in heliospheric plasmas using field-particle correlations, Astrophys. J. Lett. **826**, L30 (2016).
[45] G. G. Howes, K. G. Klein, and T. C. Li, Diagnosing collisionless energy transfer using field-particle correlations: Vlasov–Poisson plasmas, J. Plasma Phys. **83**, 705830102 (2017).
[46] K. G. Klein, G. G. Howes, and J. M. TenBarge, Diagnosing collisionless energy transfer using field-particle correlations: Gyrokinetic turbulence, J. Plasma Phys. **83**, 535830401 (2017).
[47] K. G. Klein, Characterizing fluid and kinetic instabilities using field-particle correlations on single-point time series, Phys. Plasmas **24**, 055901 (2017).
[48] C. H. K. Chen, K. G. Klein, and G. G. Howes, Evidence for electron Landau damping in space plasma turbulence, Nat. Commun. **10**, 740 (2019).
[49] T. C. Li, G. G. Howes, K. G. Klein, Y.-H. Liu, and J. M. TenBarge, Collisionless energy transfer in kinetic turbulence: Field-particle correlations in Fourier space, J. Plasma Phys. **85**, 905850406 (2019).
[50] K. G. Klein, G. G. Howes, J. M. TenBarge, and F. Valentini, Diagnosing collisionless energy transfer using field-particle correlations: Alfvén-ion cyclotron turbulence, J. Plasma Phys. **86**, 905860402 (2020).
[51] J. Juno, G. G. Howes, J. M. TenBarge, L. B. Wilson, A. Spitkovsky, D. Caprioli, K. G. Klein, and A. Hakim, A field-particle correlation analysis of a perpendicular magnetized collisionless shock, J. Plasma Phys. **87**, 905870316 (2021).
[52] J. Verniero, G. Howes, D. Stewart, and K. Klein, Patch: Particle arrival time correlation for heliophysics, J. Geophys. Res. **126**, e2020JA028940 (2021).
[53] P. Montag and G. G. Howes, A field-particle correlation analysis of magnetic pumping, Phys. Plasmas **29**, 032901 (2022).
[54] L. Boltzmann, Über die beziehung dem zweiten haubtsatze der mechanischen wärmetheorie und der wahrscheinlichkeitsrechnung resp. dem sätzen über das wäarmegleichgewicht, *Wiener Berichte* 76, 373 (1877), in (Boltzmann, 1909), Vol. II, paper 42.
[55] B. C. Eu, Boltzmann entropy, relative entropy, and related quantities in thermodynamic space, J. Chem. Phys. **102**, 7169 (1995).
[56] B. Chan Eu, Relative Boltzmann entropy, evolution equations for fluctuations of thermodynamic intensive variables, and a statistical mechanical representation of the zeroth law of thermodynamics, J. Chem. Phys. **125**, 064110 (2006).
[57] G. L. Eyink, Cascades and Dissipative Anomalies in Nearly Collisionless Plasma Turbulence, Phys. Rev. X **8**, 041020 (2018).
[58] C. Mouhot and C. Villani, On Landau damping, Acta Math. **207**, 29 (2011).
[59] H. Liang, P. A. Cassak, S. Servidio, M. A. Shay, J. F. Drake, M. Swisdak, M. R. Argall, J. C. Dorelli, E. E. Scime, W. H. Matthaeus, V. Roytershteyn, and G. L. Delzanno, Decomposition of plasma kinetic entropy into position and velocity space and the use of kinetic entropy in particle-in-cell simulations, Phys. Plasmas **26**, 082903 (2019).
[60] H. Grad, On Boltzmann's H-theorem, J. Soc. Ind. Appl. Math. **13**, 259 (1965).
[61] S. Floerchinger and T. Haas, Thermodynamics from relative entropy, Phys. Rev. E **102**, 052117 (2020).
[62] L. Boltzmann, Weitere studien über das wärmegleichgewicht unter gasmolekülen, *Wiener Berichte* 66, 275 (1872), in (Boltzmann, 1909), Vol. I, paper 23.
[63] H. Liang, M. H. Barbhuiya, P. A. Cassak, O. Pezzi, S. Servidio, F. Valentini, and G. P. Zank, Kinetic entropy-based measures of distribution function non-Maxwellianity: Theory and simulations, J. Plasma Phys. **86**, 825860502 (2020).
[64] M. R. Argall, M. H. Barbhuiya, P. A. Cassak, S. Wang, J. Shuster, H. Liang, D. J. Gershman, R. B. Torbert, and

J. L. Burch, Theory, observations, and simulations of kinetic entropy in a magnetotail electron diffusion region, Phys. Plasmas **29**, 022902 (2022).
[65] See Supplemental Material at http://link.aps.org/supplemental/10.1103/PhysRevLett.130.085201 for detailed derivations of some expressions in this Letter, an heuristic example of relative energy per particle, a description of the numerical simulation setup and methodology, and an extensive comparison of the present research with previous work, which includes Refs. [66–88].
[66] W. Grandy, Time evolution in macroscopic systems. II. The entropy, Found. Phys. **34**, 21 (2004).
[67] S. Kullback and R. A. Leibler, On information and sufficiency, Ann. Math. Stat. **22**, 79 (1951).
[68] E. T. Jaynes, Information theory and statistical mechanics, in *Statistical Physics*, edited by K. Ford (Benjamin, New York, 1963), p. 181.
[69] R. J. Diperna, Uniqueness of solutions to hyperbolic conservation laws, Indiana University mathematics Journal **28**, 137 (1979).
[70] C. M. Dafermos, The second law of thermodynamics and stability, Arch. Ration. Mech. Anal. **70**, 167 (1979).
[71] V. Vedral, The role of relative entropy in quantum information theory, Rev. Mod. Phys. **74**, 197 (2002).
[72] J. C. Robertson, E. W. Tallman, and C. H. Whiteman, Forecasting using relative entropy, J. Money Credit Bank. **37**, 383 (2005).
[73] A. E. Tzavaras, Relative entropy in hyperbolic relaxation, Commun. Math. Sci. **3**, 119 (2005).
[74] M. S. Shell, The relative entropy is fundamental to multiscale and inverse thermodynamic problems, J. Chem. Phys. **129**, 144108 (2008).
[75] F. Berthelin, A. E. Tzavaras, and A. Vasseur, From discrete velocity Boltzmann equations to gas dynamics before shocks, J. Stat. Phys. **135**, 153 (2009).
[76] J. C. Baez and B. S. Pollard, Relative entropy in biological systems, Entropy **18**, 46 (2016).
[77] G. F. Chew, M. L. Goldberger, and F. E. Low, The Boltzmann equation and the one-fluid hydromagnetic equations in the absence of particle collisions, Proc. R. Soc. A **236**, 112 (1956).
[78] M. Hesse and J. Birn, MHD modeling of magnetotail instability for anisotropic pressure, J. Geophys. Res. **97**, 10643 (1992).
[79] A. Zeiler, D. Biskamp, J. F. Drake, B. N. Rogers, M. A. Shay, and M. Scholer, Three-dimensional particle simulations of collisionless magnetic reconnection, J. Geophys. Res. **107**, 1230 (2002).
[80] C. K. Birdsall and A. B. Langdon, *Plasma Physics via Computer Simulation* (Institute of Physics Publishing, Philadelphia, 1991), Chap. 15.
[81] P. N. Guzdar, J. F. Drake, D. McCarthy, A. B. Hassam, and C. S. Liu, Three-dimensional fluid simulations of the nonlinear drift-resistive ballooning modes in tokamak edge plasmas, Phys. Fluids B **5**, 3712 (1993).
[82] U. Trottenberg, C. W. Oosterlee, and A. Schuller, *Multigrid* (Academic Press, San Diego, 2000).
[83] H. Liang, P. A. Cassak, M. Swisdak, and S. Servidio, Estimating effective collision frequency and kinetic entropy uncertainty in particle-in-cell simulations, J. Phys. Conf. Ser. **1620**, 012009 (2020).
[84] G. G. Howes, A. J. McCubbin, and K. G. Klein, Spatially localized particle energization by Landau damping in current sheets produced by strong Alfvén wave collisions, J. Plasma Phys. **84**, 905840105 (2018).
[85] V. Zhdankin, Nonthermal particle acceleration from maximum entropy in collisionless plasmas, arXiv:2203.13054.
[86] J. J. Sakurai, *Modern Quantum Mechanics (Revised Ed.)* (Addison-Wesley, Reading, MA, 1994).
[87] J. Von Neumann, Thermodynamik quantenmechanischer gesamtheiten, Nachrichten von der Gesellschaft der Wissenschaften zu Göttingen, Mathematisch-Physikalische Klasse **1927**, 273 (1927).
[88] D. A. Lidar, Lecture notes on the theory of open quantum systems, arXiv:1902.00967v2.
[89] R. L. Kaufmann and W. R. Paterson, Boltzmann *h* function and entropy in the plasma sheet, J. Geophys. Res. **114**, A00D04 (2009).
[90] T. W. Speiser, Particle trajectories in model current sheets: 1. Analytical solutions, J. Geophys. Res. **70**, 4219 (1965).
[91] J. Ng, J. Egedal, A. Le, W. Daughton, and L.-J. Chen, Kinetic Structure of the Electron Diffusion Region in Antiparallel Magnetic Reconnection, Phys. Rev. Lett. **106**, 065002 (2011).
[92] J. R. Shuster, L.-J. Chen, W. S. Daughton, L. C. Lee, K. H. Lee, N. Bessho, R. B. Torbert, G. Li, and M. R. Argall, Highly structured electron anisotropy in collisionless reconnection exhausts, Geophys. Res. Lett. **41**, 5389 (2014).
[93] S. Wang, L. Chen, N. Bessho, L. M. Kistler, J. R. Shuster, and R. Guo, Electron heating in the exhaust of magnetic reconnection with negligible guide field, J. Geophys. Res. **121**, 2104 (2016).
[94] M. H. Barbhuiya, P. Cassak, M. Shay, V. Roytershteyn, M. Swisdak, A. Caspi, A. Runov, and H. Liang, Scaling of electron heating by magnetization during reconnection and applications to dipolarization fronts and super-hot solar flares, J. Geophys. Res. **127**, e2022JA030610 (2022).
[95] J. L. Burch, T. E. Moore, R. B. Torbert, and B. L. Giles, Magnetospheric multiscale overview and science objectives, Space Sci. Rev. **199**, 5 (2016).
[96] C. Pollock *et al.*, Fast plasma investigation for magnetospheric multiscale, Space Sci. Rev. **199**, 331 (2016).
[97] J. R. Shuster *et al.*, MMS measurements of the Vlasov equation: Probing the electron pressure divergence within thin current sheets, Geophys. Res. Lett. **46**, 7862 (2019).
[98] J. R. Shuster, D. J. Gershman, J. C. Dorelli, B. L. Giles, N. B. S. Wang, L.-J. Chen, P. A. Cassak, S. J. Schwartz, R. E. Denton, V. M. Uritsky, W. R. Paterson, C. Schiff, A. F. Viñas, J. Ng, L. A. Avanov, D. E. da Silva, and R. B. Torbert, Structures in the terms of the Vlasov equation observed at Earth's magnetopause, Nat. Phys. **17**, 1056 (2021).
[99] B. Laperre, J. Amaya, and G. Lapenta, Identification of high order closure terms from fully kinetic simulations using machine learning, Phys. Plasmas **29**, 032706 (2022).
[100] S. J. Aarseth and S. J. Aarseth, *Gravitational N-Body Simulations: Tools and Algorithms* (Cambridge University Press, Cambridge, England, 2003).

[101] M. Karplus and G. A. Petsko, Molecular dynamics simulations in biology, Nature (London) **347**, 631 (1990).
[102] G. Schaller, *Open Quantum Systems far from Equilibrium* (Springer International Publishing, New York, 2014).
[103] V. Zhdankin, Generalized Entropy Production in Collisionless Plasma Flows and Turbulence, Phys. Rev. X **12**, 031011 (2022).
[104] D. Lynden-Bell, Statistical mechanics of violent relaxation in stellar systems, Mon. Not. R. Astron. Soc. **136**, 101 (1967).
[105] G. Livadiotis, Thermodynamic origin of kappa distributions, Europhys. Lett. **122**, 50001 (2018).
[106] P. A. Cassak, M. H. Barbhuiya, H. Liang, and M. R. Argall, Simulation dataset, Zenodo, 10.5281/zenodo.5847092 (2023).